Unsaturated Flow in a Centrifugal Field: Measurement of Hydraulic Conductivity and Testing of Darcy's Law

J. R. NIMMO, J. RUBIN, AND D. P. HAMMERMEISTER

U.S. Geological Survey, Menlo Park, California

A method has been developed to establish steady state flow of water in an unsaturated soil sample spinning in a centrifuge. Theoretical analysis predicts moisture conditions in the sample that depend strongly on soil type and certain operating parameters. For Oakley sand, measurements of flux, water content, and matric potential during and after centrifugation verify that steady state flow can be achieved. Experiments have confirmed the theoretical prediction of a nearly uniform moisture distribution for this medium and have demonstrated that the flow can be effectively one-dimensional. The method was used for steady state measurements of hydraulic conductivity K for relatively dry soil, giving values as low as 7.6×10^{-11} m/s with data obtained in a few hours. Darcy's law was tested by measuring K for different centrifugal driving forces but with the same water content. For the sand at a bulk density of 1.82 Mg/m^3 and 27% saturation, results were consistent with Darcy's law for K equal to 5.22×10^{-10} m/s and forces ranging from 216 to 1650 times normal gravity.

INTRODUCTION

Every study of water movement in unsaturated porous media makes use of some sort of driving force, usually gravity or gradients of matric potential ψ. For some purposes the use of centrifugal force has great advantages. Like gravity, centrifugal force is a body force, so it works independently of ψ gradients. This fact is important with unsaturated soils, where ψ gradients necessitate gradients of water content θ and hydraulic conductivity K, thus introducing a complexity which is undesirable for many purposes. Like gradients of ψ, centrifugal force can have very large magnitudes. This is advantageous whenever K is small enough that gravity-driven experiments become impractical or impossible because of the time required. A further advantage of centrifugal force is that it is easy to adjust simply by changing the speed of rotation.

Centrifugal force has been used in a variety of applications to unsaturated porous media, beginning with the "moisture equivalent" studies of *Briggs and McLane* [1907]. Later developments by *Russell and Richards* [1938] and *Hassler and Brunner* [1945] resulted in practical techniques, still widely used in the oil industry, for measuring liquid-retention properties. *Bear et al.* [1984] have presented a theoretical analysis of the approach to equilibrium of liquid in a deformable porous medium in a centrifugal field. *Stewart et al.* [1967], *Alemi et al.* [1976], and *Hagoort* [1980] have used centrifugal force in measuring K. One of these techniques, a variation of the moment method, measures the redistribution of water in a soil column after it has been brought to a known ψ distribution by equilibration in a centrifugal field. The other, a variation of the outflow method, calculates K using measurements of the volume of water flowing out as a function of time from a sample undergoing drainage in a centrifugal field. While centrifugal force can improve the speed and convenience of these transient methods, it does not remove their basic limitations.

For accurate measurement of K in unsaturated porous media, steady state methods are usually preferable to transient methods. The time dependence of relevant quantities such as

θ, ψ, and flux density q means that more kinds and a much greater quantity of data are required under transient than under steady conditions. In general there are many crucial data that are not measured directly and so must be inferred using approximations and assumptions that may not be completely justified. The simplicity and directness of steady state methods usually produces greater accuracy. The chief limitation of steady state methods is that they are slow, more time being required for lower K values. Practical considerations usually limit the application of steady state methods to the large K values of nearly saturated media. The use of centrifugal forces thousands of times greater than normal gravity drastically reduces the time required for these measurements and thereby increases the range of measurable conductivity. The first objective of the present study was to show, using relatively simple apparatus, that it is possible to achieve steady state unsaturated flow in a centrifugal field and to use such flow to measure low K values rapidly.

Conventional steady state methods for K measurement were pioneered by *Richards* [1931], who drove the flow by gravity in combination with a constant pressure gradient applied by ceramic plates on the top and bottom of a soil column. A drawback usually limiting the accuracy of this method is that K is not uniform within the sample; K varies with the water-content distribution associated with the ψ profile. It is possible to reduce this nonuniformity using a modified procedure described by *Mualem and Klute* [1984] or to avoid it by using the measurement technique of *Childs and Collis-George* [1950]. In a long, initially saturated soil column with a water table at the bottom and constant flux applied at the top, Childs and Collis-George established a region of uniform water content where the flow was driven only by gravity. Slow flow rates make this method applicable only in fairly wet media. Another method, developed theoretically by *Rubin and Steinhardt* [1963] and *Youngs* [1964] and experimentally by Youngs as well as *Rubin et al.* [1964], uses an initially dry column in which infiltration at a constant rate under gravity eventually creates a downward expanding region near the top in which θ is essentially uniform and unchanging. A variation of this method, for which the theoretical basis was pioneered by *Kisch* [1959] and developed into an experimental method by *Hillel and Gardner* [1970], makes use of a constant head of
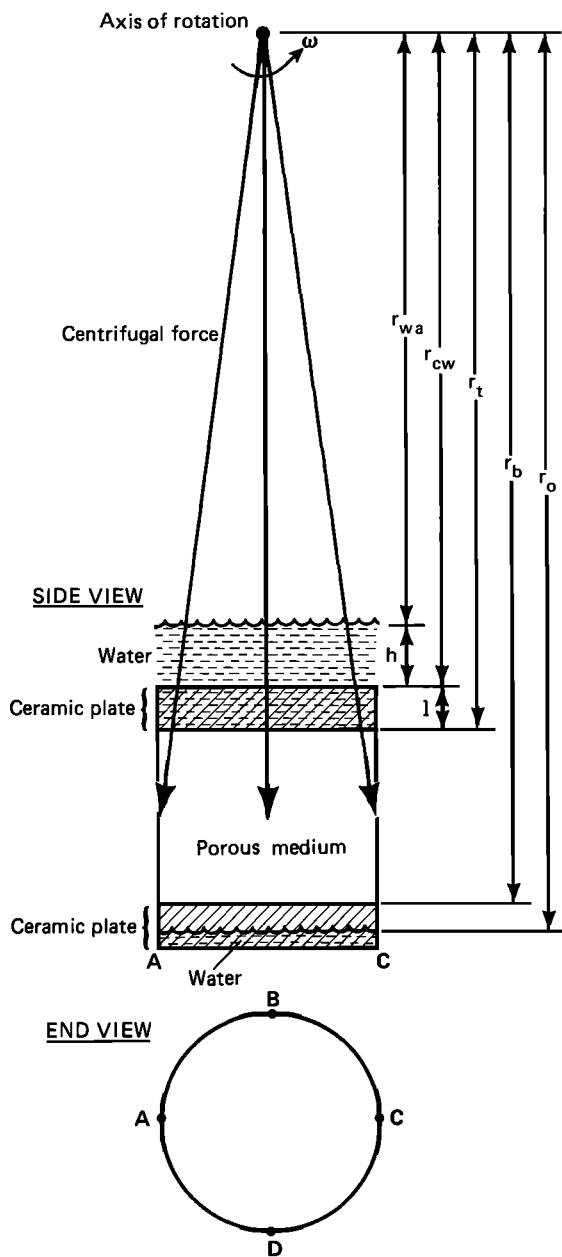
Fig. 1. Cross-sectional views (to scale) of a sample with porous plates and free-water levels in a centrifugal field. The water-air surfaces would be curved in the actual situation, but they are shown here as flat, so that the definitions of dimensions would be clear.

water above an impeding layer of porous material on top of the soil. The impeding layer, usually a crust or porous plate, is selected to have a saturated K smaller than that of the sample, so that with water flowing, the sample will remain unsaturated. Lower K values for the impeding layer will result in a drier medium and a lower measured value of K.

The adaptation of the steady state method for use in a centrifuge requires that all apparatus fit into a small bucket and withstand great mechanical stresses. These requirements rule out commercially available pumps, pressure regulators, and transducers. It is possible, though, to employ constant water levels and impeding layers to regulate the flow. As is shown later, the matric potential cannot be uniform when a centrifugal force is present, but this does not make steady state flow impossible.

The second objective of this study is to test Darcy's law. Written as

$$q = -K\nabla\Phi \qquad (1)$$

where q is flux density and Φ the total hydraulic potential, Darcy's law is simply the statement that flux is directly proportional to driving force. A rigorous test of this law requires accurate flux measurements while driving forces are varied, with all other experimental conditions maintained essentially constant. Although transient methods have been employed in such tests [e.g., Swartzendruber, 1963; Watson, 1966; Thames and Evans, 1968], the inherent complexity of these techniques makes it difficult to ensure that factors other than the driving force are indeed constant. The comparison of flux for different driving forces may have to be made for different parts of the sample or for different matric potential gradients. Another problem with transient methods is that they may not be accurate enough to detect small deviations. The more direct and simple steady state methods are better suited to the task of testing Darcy's law under conditions effectively identical except for driving force.

The first steady state test of Darcy's law was by Childs and Collis-George [1950], using their method of gravity-driven flux through a region of constant moisture. By tilting the column, Childs and Collis-George varied the driving force by a factor of 2. Experimental results for two sand fractions supported Darcy's law, but the test suffered from two limitations: the soil was fairly wet ($\psi = -2.3$ kPa) and the driving force was varied only over the limited range of 0.5–1.0 g.

Hadas [1964] and Olson and Swartzendruber [1968] used Richards' [1931] flow-cell method with various applied pressure gradients to test Darcy's law. Although this technique permits somewhat greater force variations (from 0.5 to 14 g in Hadas's work) than the column-tilting method, it introduces the problem of nonuniform moisture profiles, which are different for different gradients. Hadas dealt with this problem by using very short columns, while Olson and Swartzendruber compensated in their mathematical treatment of the data. Hadas found small deviations from Darcy's law for clay and loess samples, but his experiments have been criticized for several possible weaknesses: (1) the potential gradient within the sample was not measured directly, (2) the differences in moisture profiles associated with the different gradients may have affected the K measurement (made for the sample as a whole) due to the nonlinearity and hysteresis of $K(\psi)$, and (3) different samples, with thicknesses varying from 5 to 15 mm, were used for different portions of the range of driving force. Olson and Swartzendruber found in general that Darcy's law was upheld for mixtures of sand and ground silica with and without kaolinite. Slight deviations were found in a few cases, however. Although their method reduced or eliminated some of the weaknesses of Hadas's experiment, it was subject to approximations in the much more complicated mathematical analysis and to problems resulting from variations in water-content profile over the 100-mm column length.

Use of a centrifuge steady state method to test Darcy's law can remove three of the usual limitations on such experiments: (1) the test can be extended to the low K values of a relatively dry porous medium, (2) the driving force can be varied without necessarily affecting the moisture gradient, and (3) the Darcy proportionality can be tested over a much greater range of driving force. But first it must be shown that
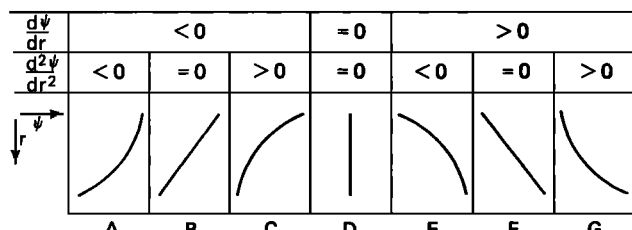
Fig. 2. Hypothetical shape elements for segments of the steady state $\psi(r)$ profile for a porous medium in a centrifugal field.

steady state flow is possible in a centrifugal field, and then that essentially identical moisture conditions can be maintained when the centrifugal force is varied.

THEORY

To understand the validity, limitations, and generality of the experimental results of this study, it is necessary to consider the theory of unsaturated water flow in a centrifugal field. The key questions are what physical quantities must be measured to determine $K(\psi)$ or $K(\theta)$ and what experimental conditions best facilitate the required measurements. Of primary importance is the nature of the moisture distribution in the sample, specifically the shape of the ψ profile, during steady state flow.

Figure 1 illustrates the situation in which water flows through a porous medium in a centrifugal field with constant boundary conditions established using constant water levels and porous ceramic plates. The water is driven by the centrifugal force per unit volume $\rho\omega^2 r$, where ρ is the density of water, ω is the angular speed of rotation, and r is the distance from the axis. Eventually the flow will become steady so that Darcy's law may suffice to describe the flow. For one-dimensional flow, neglecting gravity and hysteresis, Darcy's law can be expressed as

$$q = -K(\psi)\left[\frac{d\psi}{dr} - \rho\omega^2 r\right] \qquad (2)$$

The determination of $K(\psi)$ thus requires a measurement of q and the two terms of driving force.

The shape of the $\psi(r)$ profile is crucial in measuring the $d\psi/dr$ term of driving force in (2). The simplest case is that of essentially constant $\psi(r)$. Since $d\psi/dr$ would be negligible and
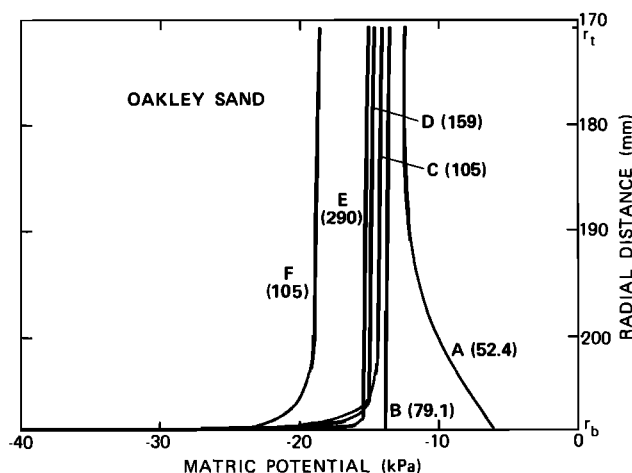

Fig. 3. Matric potential profiles computed by a one-dimensional numerical model for Oakley sand undergoing steady state flow in a centrifugal field. The ordinate is the radial distance from the center of rotation. Numbers in parentheses are the angular speeds in s^{-1}.
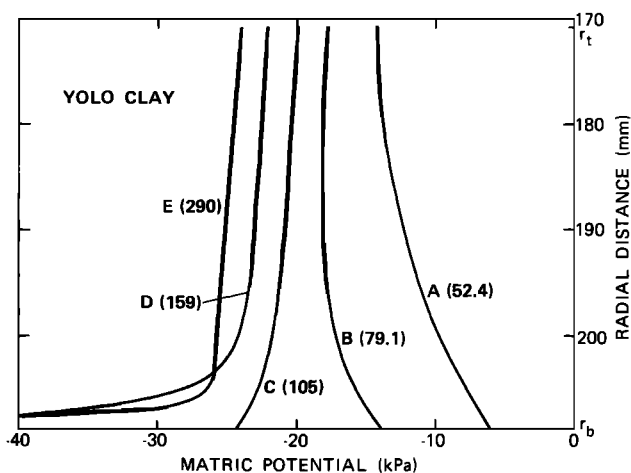

Fig. 4. Matric potential profiles computed for Yolo clay undergoing steady state flow in a centrifugal field at the angular speeds indicated by the numbers in parentheses.

θ effectively constant, $K(\psi)$ could be determined with a ψ measurement at a single point, and $K(\theta)$ could be determined without any measurement of ψ. One K value would be obtained in each experimental run. For a $\psi(r)$ profile that is linear but not constant, two measured (r, ψ) points would be required, but K values could then be calculated over the range of ψ covered by the linear profile. A nonlinear $\psi(r)$ profile would also permit K calculations over a range of ψ, but more than two measured (r, ψ) points would be required, and $d\psi/dr$ values would have to be estimated at selected points. Because experiments are simpler and easier for profiles that are essentially linear or constant, it is desirable to predict the conditions that might lead to such profiles.

Figure 2 shows a complete set of shape elements, hypothetical segments of $\psi(r)$ curves classified according to the signs of the first and second derivatives of $\psi(r)$. Any profile can be considered as a set of successive shape elements. Several reasonable assumptions about the medium and the nature of the flow lead to various conclusions concerning which shape elements may exist and how they may combine. Appendix A presents justifications for the most important of these conclusions. In brief, it is shown that shape elements D, E, and F (Figure 2) are impossible, that B is possible only for a particular form of the $K(\psi)$ function, and that for a sufficiently long column, G can exist only in combination with C. It is also shown that elements A and C can approximate elements B and D. Since the experimentally simple cases of linear or constant $\psi(r)$ are represented by elements B and D, it is desirable to seek cases where these shapes are approximated over a large fraction of the profile.

For quantitative predictions of the $\psi(r)$ profile during steady state flow, it is possible to solve (2) directly for given q, $K(\psi)$, and ψ_b, where ψ_b is the boundary condition $\psi(r_b)$, r_b being the value of r at the bottom of the sample. We have developed a model for solving this problem using the fourth-order Runge-Kutta method [Henrici, 1964] with $K(\psi)$ computed by the empirical relation

$$K(\psi) = \frac{K_{sat}}{(\psi/\psi_0)^n + 1} \qquad (3)$$

which was first used by Gardner [1964].

Figures 3 and 4 show $\psi(r)$ profiles for Oakley sand and Yolo light clay calculated by the one-dimensional model using

TABLE 1. Parameter Values Used in (3)

Parameter	Oakley Sand	Yolo Clay
K_{sat}, m/s	2.920×10^{-5}	1.1157×10^{-7}
ψ_0, kPa	-1.449	-1.961
n	4.5398	2

Values for Oakley sand were obtained by the gravity-driven steady state method (K_{sat}) and by least squares fit to measurements by the centrifuge steady state method (ψ_0 and n). Values for Yolo light clay were those previously used by Rubin [1968].

the Gardner-formula parameter values in Table 1 and values of input parameters ω, q, and ψ_b that can be achieved with the apparatus described in this paper. Relevant apparatus dimensions are given in Table 2, and procedures for determing realistic parameter values are described below. Table 3 lists the input parameter values and selected results of the computations. To show the influence of ψ_b, the five curves in Figure 5 were computed with five different ψ_b values but with all other input parameters the same.

Most of the curves in Figures 3–5 have an upper region of nearly constant ψ gradient. Below this region is a zone where the ψ gradient varies as $\psi(r)$ curves to meet the boundary condition ψ_b. Figure 6 shows the gradients of matric, centrifugal, and total potential versus r for curve C of Figure 3, showing that over most of the column length, the centrifugal potential gradient overwhelms the matric potential gradient. For each of the profiles the ψ gradient of the upper region has the values predicted by formulas in Appendix A, about -20 kPa/m for Oakley sand and -60 kPa/m for Yolo clay. The length of the "constant-gradient" region (Table 3, columns 6 and 9) depends straightforwardly on ω and soil type, being greater on the whole for greater speed and for soil with a more drastic dependence of K on ψ. This length also depends on ψ_b, but as is clear from Figure 5, the effect is to lengthen the constant-gradient region only for the case when ψ_b is close to the ψ values present in that region. The fact that the curves in Figure 5 come together in the upper region is consistent with the prediction, presented in Appendix A, that for cases of identical q and ω the value of ψ_b generally has little influence above a certain point in the profile. The effect of ψ_b is also clear for curve B of Figure 3, for which ω was chosen in such a way that ψ_b would have a value close to that which maximizes the length of the constant-gradient region. For the Oakley sand curves C–E in Figure 3, because the lower region of the profile is short and highly curved, ψ_b has little influence on ψ_t and the average ψ.

In most of the steady state profiles of interest, moisture conditions are such that θ changes little with ψ. Therefore θ has less variation with r than does ψ. Taking curve C of Figure 3 as an example, the $\theta(r)$ profile computed from $\psi(r)$ and the water-retention curve show that the Oakley θ varies by only 1.2% of its average value over the constant-gradient region, while ψ varies by 5.0%. For this curve the average water content in the constant-gradient region is 0.0805 m³ water/m³, very close to the average θ of 0.0797 for the whole sample. For profiles with longer regions of constant gradient, the comparison would be even closer. Thus for many steady state profiles, θ varies significantly in such a small portion of the column that a measurement of the whole-sample average adequately characterizes the profile.

To obtain experimentally useful predictions with the nu-

merical model, it is necessary to produce realistic estimates of the parameters q and ψ_b. Referring to Figure 1, q is determined primarily by the conductance of the upper ceramic plate and the height h of water above this plate. Appendix B presents formulas for estimating q from these and other characteristics of the apparatus. The boundary condition ψ_b is determined by the suction generated by the free-water surface at r_0, below the top of the lower ceramic plate. If this plate has negligible impedance, the pressure distribution within it will be described by the equilibrium (zero-flux) profile [Veihmeyer et al., 1924; Gardner, 1937]:

$$\psi(r) = \frac{\rho\omega^2}{2}(r^2 - r_0^2) \qquad (4)$$

the value of ψ_b is computed simply as $\psi(r_b)$ in (4). For bottom plates with conductivity 2.2×10^{-7} m/s, the error in ψ_b due to the nonzero impedance is about 0.5% for the curves of Figures 3 and 4.

Because the input parameters for the curves in Figures 3 and 4 were determined by the selected ceramic plate conductivities, they illustrate the effect of different ω values with the same plate (curves A–E in both figures) and different plates with the same ω (curves C and F in Figure 3). These effects are quantified in Table 3. For the Oakley sand curves (Figure 3), it is clear that for speeds of 79.1 s^{-1} or more, ω has relatively slight influence on ψ_t (12%) and on the average ψ value. Curve F compared with C shows that a relatively small (factor of 3.5) difference in q as determined by different ceramic plates has a significant effect on the average ψ. Yolo clay, with its lower K_{sat} and less drastic dependence of K on ψ, is more sensitive than Oakley sand to ω, ψ_b, and K_c. Even so, Yolo shows only a 66% difference in ψ_t for more than a fivefold increase of ω and a 12-fold increase of q.

Besides its r dependence and large magnitude, the centrifugal force differs from gravity in ways that complicate the steady flow situation. Water in the sample is subject to Coriolis forces and forces due to angular acceleration when the centrifuge starts or stops. These effects, though, can easily be shown to be negligible for the flow rates encountered in unsaturated soil. A more serious problem is the angular divergence of the centrifugal force. As Figure 1 illustrates, this force is always directed along a radius of the centrifuge, so it is not parallel to the axis of a cylindrical sample at most points. The resulting curvature of the free-water surfaces and the existence of force components perpendicular to the walls of the sample create a tendency for the soil to be wetter and the flux to be greater near certain portions of the outer boundary. This effect thus violates the one-dimensional assumption used in K calculations. It is especially important at higher speeds, where the nonaxial components of centrifugal force are greater. Where the divergence effect is significant, the total flux will be greater than for the case where moisture conditions are laterally uniform.

If it can be verified experimentally that steady state flow can be established in a centrifugal field, that such flow can be

TABLE 2. Radii in Millimeters From the Axis of Rotation to Various Points Indicated in Figure 1

r_{wa}	r_{cw}	r_t	r_b	r_0
153.2	161.7	170.7	208.7	211.9

The values can be obtained with the apparatus of Figure 7.

TABLE 3. Parameter Values and Resulting Characteristics of Curves in Figures 3 and 4

			Oakley Sand (Figure 3)			Yolo Clay (Figure 4)		
Curve	Input ω, s^{-1}	Input ψ_b, kPa	Input q, 10^{-8} m/s	Result ψ_t, kPa	Result Constant-Gradient Length Fraction	Input q, 10^{-8} m/s	Result ψ_t, kPa	Result Constant-Gradient Length Fraction
a	52.4	−6.12	8.759	−12.3	0.08	9.677	−14.3	0.00
b	79.1	−13.9	13.76	−13.3	0.98	15.79	−17.8	0.11
c	105	−24.5	19.63	−13.9	0.74	22.13	−19.8	0.47
d	159	−56.5	38.00	−14.5	0.87	41.17	−21.9	0.58
e	290	−188.	110.8	−14.9	0.97	114.6	−23.8	0.82
f	105	−24.5	5.647	−18.4	0.74			

The constant-gradient length fraction is defined as the fraction of the 38-mm column length over which the gradient is within 10% of its value at the top of the sample.

effectively one-dimensional, and that the flux during centrifugation can be accurately measured, then the possibility of an accurate K measurement depends on the $\psi(r)$ profile. Because the case of effectively constant $\psi(r)$ has probably the greatest experimental value, the experiments of this study concentrate on verifying that such a profile is possible and can be used in K measurements and tests of Darcy's law.

EXPERIMENTAL METHOD

The method developed for determining K by establishing and measuring steady state unsaturated flow in a centrifugal field (patent applied for, ser. 901,360) uses the apparatus shown in Figure 7. The assembled components fit into a 1-L bucket and can be centrifuged at speeds up to 320 s^{-1}. With the sample at about 200 mm from the centrifuge axis, the driving force at the maximum speed is about 2000 g.

The cylindrical sample, 50 mm in diameter and about 38 mm high, has ceramic plates on both ends for the establishment of boundary conditions. A constant water level is maintained in reservoir 2, the constant-head reservoir, immediately above the ceramic plate (referred to as the "applicator plate") that sits on top of the sample. The applicator plate is supported only by the underlying sample, so contact is not lost if the sample becomes further compacted. Water is continuously supplied to reservoir 2 from reservoir 1, the supply reservoir,

at a rate somewhat greater than the flux through the soil. Overflow through a hole in the side of reservoir 2 determines the height of the water surface above the applicator plate. Overflow collects in reservoir 3, the upper overflow reservoir. The pressure just above the applicator plate can be varied by as much as a factor of 1.6 by unplugging one of several overflow holes at various heights. The applicator plate has a conductivity low enough to establish the desired unsaturated condition of the soil.

At the bottom of the soil, a constant matric potential is established by means of a free-water surface slightly above the bottom of the lower ceramic plate. This plate sits in a shallow dish; water flowing out from the soil accumulates in this dish until it flows over the lip. Thus the height of the lip determines the height of the free-water surface. The capacity of the dish is small (about 0.1 mL), so that when the centrifuge stops, little water is available to flow back up into the soil. Water leaving the bottom overflow dish ends up in reservoir 4, the lower overflow reservoir.

Each steady state measurement of K started with saturated soil, which was previously compacted at 1950 g to the point where further centrifugation over the force range used in measurements would cause little change in bulk density. The water used to saturate the soil and to fill reservoirs 1 and 2 was a deaired solution of 0.01 N CaSO$_4$ and 0.01 N CaSeO$_4$. This solution was designed to inhibit microbiological growth and to prevent changes in soil structure due to dispersion of
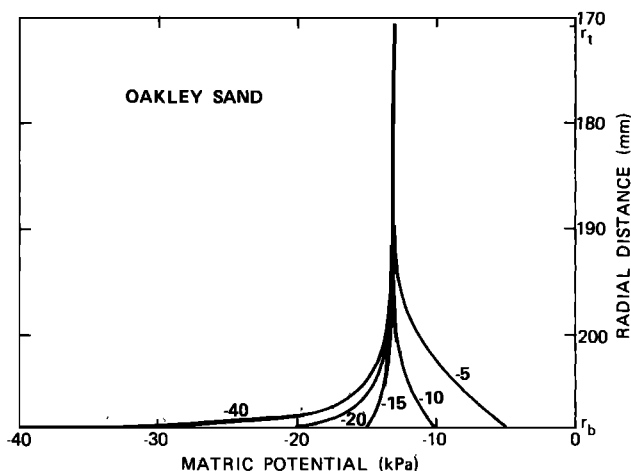

Fig. 5. Matric potential profiles computed for Oakley sand undergoing steady state flow in a centrifugal field. The curves were computed with $\omega = 65.9$ s^{-1}, $q = 1.174 \times 10^{-7}$ m/s, and different ψ_b values indicated next to each curve.
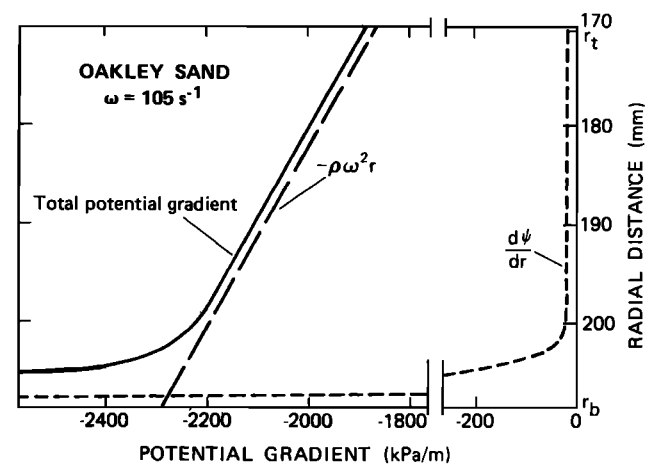

Fig. 6. Matric, centrifugal, and total potential gradients for curve C of Figure 3.

1— Supply reservoir
2— Constant-head reservoir
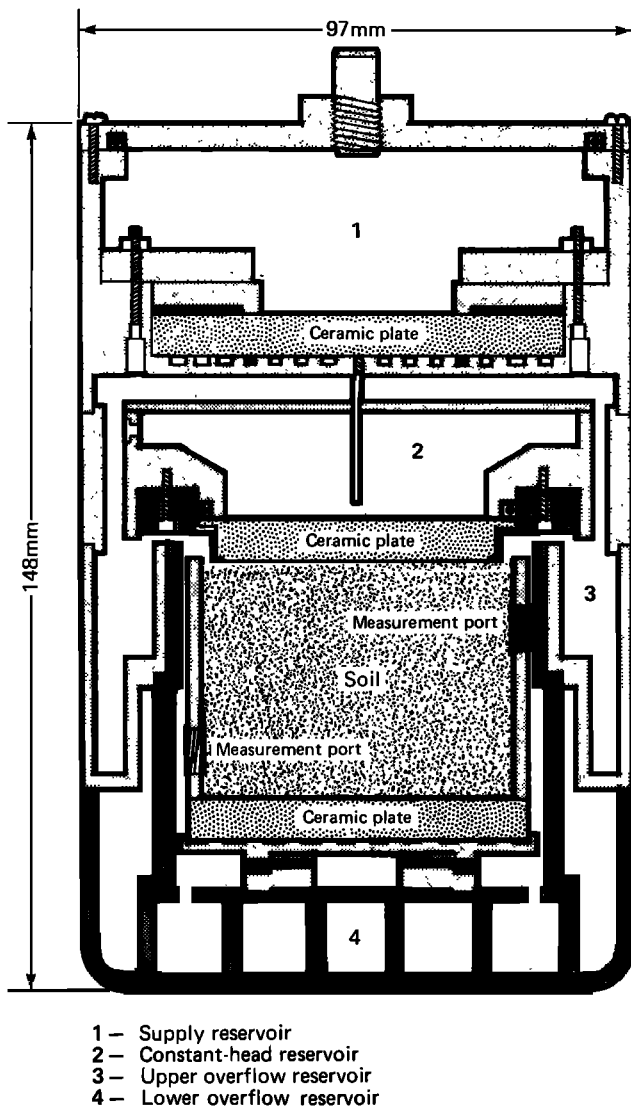3— Upper overflow reservoir
4— Lower overflow reservoir

Fig. 7. Cross-sectional view of the experimental apparatus. This assembly fits into a centrifuge bucket oriented so that the centrifugal force is directed from the top to the bottom of this diagram.

clay. To keep the rotor balanced and provide replication, two identical sets of apparatus were run simultaneously, opposite each other in the centrifuge. Air temperatures in both the laboratory and the centrifuge chamber were thermostatically controlled at 22°C. The samples were put through a series of centrifuge runs, usually with durations between 15 min and 2 hours each. Between runs, the apparatus was separated into three sections, which were individually weighed to verify and measure the steady state flow. (1) The soil and its container were weighed (with the top surface temporarily capped to reduce evaporative losses) to determine the soil's average water content. (2) The upper reservoir assembly, comprising reservoirs 1, 2, and 3, was weighed as a unit. The change in weight divided by the elapsed time of the run gives the average flux into the soil during the run. (3) Similarly, reservoir 4 and related apparatus were weighed for an indication of the flux out of the soil.

Centrifuge runs were repeated until steady state flow was verified by (1) constant average water content during a run (known from constant soil weight and also from equality of inflow and outflow) and (2) unchanging flux in two successive

runs. Figure 8 shows graphs of water content and flux density versus total time in the centrifuge, individual points representing measurements done between centrifuge runs. In this example, steady state flow was attained in about 3 hours. To attain steady state conditions for the lowest K value measured, about 8 hours of centrifugation were required. A typical interruption for weighing lasted about 10 min: 4–5 min for deceleration, about 5 min for the weighing of two sets of apparatus, and less than 1 min for acceleration. Longer interruptions were occasionally required to adjust water levels in the reservoirs.

The calculation of K using (2) requires knowledge of the flux density and also the potential gradient, both matric and centrifugal. The flux measurements based on changes in reservoir weights were corrected for flow taking place during centrifuge acceleration and deceleration, using data from steady state runs of varying duration. On a graph of volume flow versus duration of centrifuge run, a regression line fitted to the data has slope equal to the corrected flux and volume intercept equal to the amount of correction. The magnitude of the correction was typically less than 1% of the total flux. Dividing the corrected flux by the cross-sectional area of the sample yields flux density.

To determine the potential gradient, $\psi(r)$ must be measured. For this purpose we have developed three different techniques, none of which gives complete knowledge of the profile at the time of centrifugation. Only one or two of these techniques were used in any given steady state run. Considered as a whole, results of the various measurements made for a number of runs provide a reasonable picture of the $\psi(r)$ distribution.

Direct measurements of ψ were made after most steady state runs using a tensiometer. Each sample retainer has four plugged holes, designated "measurement ports" in Figure 7. For a ψ measurement the plug in a selected port was removed and the tensiometer, a thin, 6-mm diameter ceramic disk on the end of a short stainless steel tube, was brought into good contact with the soil. The pressure was read by a transducer, which had a plunger attached to the water-filled chamber, so that the approach to equilibrium could be hastened by manual adjustment. This tensiometer-transducer system was developed by *Stonestrom* [1986]. Between the end of the centrifuge runs and the first ψ measurement there was a time span of half an hour or more, during which the moisture would redistribute and alter the $\psi(r)$ profile. It was therefore necessary to extrapolate backward in time to estimate the $\psi(r)$ values existing during steady state flow.
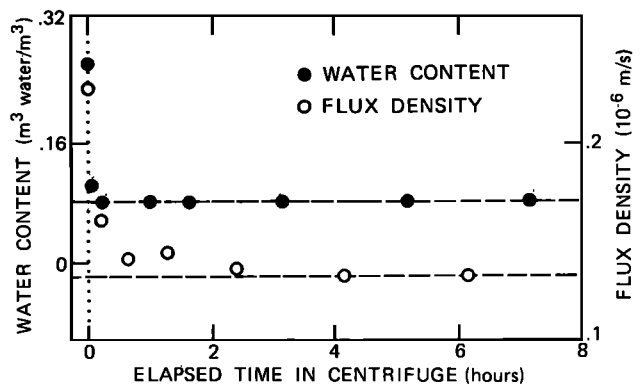

Fig. 8. Water content and flux density at the top of the sample, as functions of cumulative time of centrifugation to show the approach to steady state conditions. Measurements were done for Oakley sand at angular speed 104 s^{-1}.

To obtain a more detailed, approximate picture of the $\psi(r)$ profile with less time lag, the indirect method of gravimetrically analyzing slices of the sample was used. The procedure, carried out in a humidified chamber (to minimize evaporation), is to gradually push the sample out of its container with a piston and slice off thin portions as they are extruded. Each slice is collected separately, and its water content is determined by weighing and oven drying. The resulting $\theta(r)$ points can be converted to $\psi(r)$ using a known retention curve.

To get around the redistribution problem, a technique was developed for moisture measurement during centrifugation using the method of electrical resistance. Two flat nichrome electrodes, about 1 mm square and 3 mm apart, were placed in direct contact with the soil at one of the measurement ports. The large centrifugal force maintained a firm and steady contact between the electrodes and soil. A battery-powered solid state circuit, potted in epoxy for protection against severe mechanical stresses, was put into an adjacent centrifuge bucket and connected by wires to the electrodes. This circuit measured the time-integrated value of soil resistance during a run and recorded it to be read later when the centrifuge was stopped. This measurement was based on the output of a simple ac voltage divider with the soil resistance as one leg and a precision resistor as the other. The voltage was rectifed and applied to a voltage-to-frequency converter, pulses from which drove a digital counter. At the end of a run, the counter reading divided by the elapsed time of the run indicated the average frequency and hence the average resistance between the electrodes during the run. This device was calibrated for ψ as a function of resistance by using it in a soil column in the centrifuge without inflow, so that at equilibrium at the position of the electrode probe, ψ was known by (4).
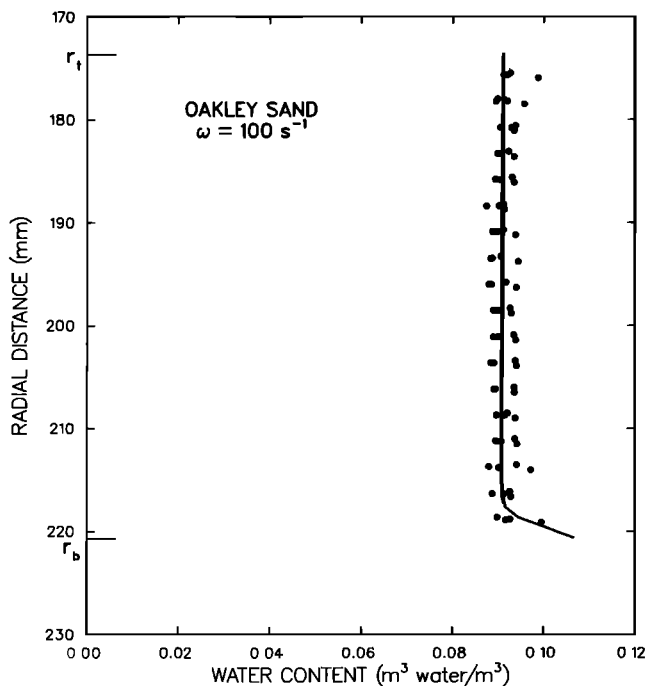

Fig. 9. Water-content measurements for 1.25-mm-thick slices of columns in which steady state flow was achieved. The points shown are from four different samples. The curve was computed by solving (2) using the one-dimensional profile model, taking the measured flux and centrifuge dimensions as input parameters. For use in the conversion of $\psi(r)$ to $\theta(r)$, the data of Table 4 were interpolated by the modified spline method of Stonestrom [1986].
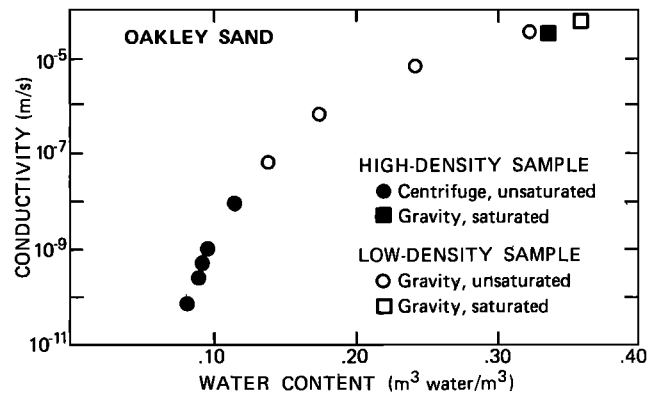

Fig. 10. Hydraulic conductivity as a function of water content for Oakley sand.

RESULTS

The steady state centrifuge method was successfully applied to Oakley sand packed by the method of Ripple et al. [1973] and compacted in the centrifuge to a bulk density of 1.82 Mg/m^3 (porosity 0.335). The clay, silt, and sand contents were 3.8%, 3.6%, and 92.6%, respectively.

The moisture profiles measured for Oakley sand were qualitatively consistent with the high-ω curves pictured in Figure 3, nearly uniform except near the lower boundary. Figure 9 shows experimental and theoretical determinations of the water-content profile after achieving steady state flow at 100 s^{-1}. The measured points fit the results of the one-dimensional profile model with a standard error of estimate 0.0025. The samples, which were destroyed in the process of making these measurements, were not used in the measurement of K or the testing of Darcy's law.

From direct measurements of matric potential, with a sensitivity of ±60 kPa/m, no measurable gradients were detected after a steady state run. As expected from theory, substantial differences in overall soil moisture were obtained only by using applicator plates of different conductivities. These two facts meant that only one value of K was obtained for each different ceramic plate material used.

The assumption of one-dimensionality was tested experimentally. The first test investigated the possibility of excessive flow on or very close to the inside wall of the sample retainer. Using modifications of the outflow assembly designed to separately collect flow down the wall and flow through the bulk of the sample, it was found that there was negligible flow at the wall during steady state conditions. The second test considered the possibility of a nonuniform moisture distribution, using the electrical resistance apparatus. Due to the divergence of forces shown in Figure 1, water flowing along the lines of force should tend to accumulate more near points A and C than near points B and D. Steady state runs were performed with the resistance probe placed alternately at points A and B. In 10 runs, ψ was significantly greater at A than at B by 5.2 ± 1.6 kPa at centrifugal accelerations of 1900 g with an average ψ for the sample of −19.6 kPa. There was no significant difference at 200 g.

Five $K(\theta)$ points obtained with steady state flow in the centrifuge are plotted (solid dots) in Figure 10. Soil conditions corresponding to these measurements are described by data in Table 2. There are five points because five different ceramic materials (Soilmoisture Equipment Co., Santa Barbara, California) were found, which could serve as applicator plates

TABLE 4. Hydraulic Conductivity Measurements for Oakley Sand
at Five Different Moisture States

Water Content, m³ water/m³	Matric Potential, kPa	Hydraulic Conductivity, m/s
0.117	-9.3 ± 0.3	$(8.7 \pm 0.6) \times 10^{-9}$
0.099	-13.0 ± 0.4	$(1.02 \pm 0.07) \times 10^{-9}$
0.092	-14.7 ± 0.4	$(5.3 \pm 0.4) \times 10^{-10}$
0.090	-17.5 ± 0.5	$(2.7 \pm 0.2) \times 10^{-10}$
0.081	-27.0 ± 0.8	$(7.6 \pm 0.5) \times 10^{-11}$.

Water content was determined from the weight of entire samples, and matric potentials were measured with tensiometers after steady flow had stopped. For each measurement of water content the error was ± 0.002 m³ water/m³.

(mention of specific brand names does not imply endorsement by the U.S. Geological Survey). The highest and lowest K values were measured with 2-bar and 15-bar air-entry-value plates, and the three middle values were obtained with 5-bar plates from different manufactured batches. The measurements compare favorably with results from two other techniques applied to essentially the same soil packed somewhat less densely. Shown for comparison in Figure 10 are data from C. Ripple and J. Rubin (private communication, 1981) obtained by constant-flux infiltration into initially dry Oakley sand with porosity 0.358. The moisture ranges of these two data sets do not overlap, so they cannot be compared directly. Both sets, though, do have some overlap with the data obtained by Stronestrom [1986] for Oakley sand with porosity 0.365 using a transient method. In each case the transient $K(\theta)$ values are greater than the steady state data by less than a factor of 2, reasonably good agreement considering the different experimental techniques.

Experimental errors (Table 4) were computed by combining estimated measurement errors on each type of primary data (time, balance readings, etc.) used in computing the results. By this method the combined random and systematic errors are $\pm 2\%$ for θ, $\pm 3\%$ for ψ, and $\pm 7\%$ for K.

The lowest K value measured, 7.6×10^{-11} m/s, probably does not represent the ultimate limit of the steady state centrifuge technique. When this measurement was done, the only experimental limitation was the availability of suitable low-conductivity ceramic plates for the top of the soil.

To test Darcy's law, flux measurements were made for various driving forces with soil moisture held as constant as possible. For nine determinations of the profile-average water content during the course of this test, the mean was 0.0916 and the standard deviation 0.0013. Assuming the one-dimensional profile model is valid (as suggested by the data in Figure 9), the essentially constant moisture distributions in Figure 3 and the nearly constant profile-average values lead to the conclusion that the θ profiles were effectively identical at the different speeds. The observed weak sensitivity of the soil moisture profile to angular speed was very fortunate for this particular experiment. Adjustments in the water level h (Figure 1) partially compensated for the slight speed dependence that does exist. The Darcy's law test was not done at the driest water content of Table 1 but rather the third driest, because the ceramic plates used to obtain this point were mechanically very strong and would work reliably over a large range of driving force. Results of the Darcy's law test appear in Figure 11. Except at the greatest force, the measured points show the direct proportionality between flux and driving force

that Darcy's law predicts. The discrepancy at 1950 g may result from experimental artifacts. The non-one-dimensional effect predicted by theory and observed with the electrical resistance apparatus at this driving force causes the flux to be greater than would be the case if moisture conditions were uniform. The line shown in the drawing is a least squares regression on all points at forces less than 1650 g. These points fall within experimental error of the line. The slope of this line indicates K equal to 5.22×10^{-10} m/s, while the quality of the fit (correlation coefficient 0.9985) and the intercept of 1.83 $\times 10^{-9}$ m/s provide strong support for Darcy's law.

DISCUSSION AND CONCLUSIONS

The theory and experiments described in this paper show that for Oakley sand, it is possible to achieve steady state, effectively one-dimensional unsaturated flow in a centrifugal field with driving forces from 200 to 1650 g. The nearly uniform moisture profiles obtained for this medium permit easy computation of hydraulic conductivity, with estimated accuracy $\pm 7\%$, from measured fluxes and the known centrifugal force. Even for K values less than 8×10^{-11} m/s, the flow measurements can be completed in 24 hours or less. Flux measurements for widely ranging driving forces, with water content essentially constant at 0.0916, strongly support Darcy's law.

The K measurement technique described here combines the advantages of simplicity and good accuracy characteristic of steady state methods with the speed and versatility afforded by the use of centrifugal force. Its chief limitation is that it applies only to compacted samples. Thus it is usable for dense sands and consolidated sediments but not for most surface soils. Although the present apparatus works very well for relatively low K values, for some media it would be difficult to apply in the wet range because the small reservoirs would be inadequate for use with large flow rates.

The method is insensitive to vapor transport due to thermal or matric-potential gradients. Thermally driven vapor flow may be important under dry, low-K conditions, but this is not an effect for which Darcy's law or the concept of hydraulic conductivity applies. Matric-potential-driven vapor flow, on the other hand, is included in the concept of isothermal K, but the magnitude of such flow is negligible under realistic conditions, as was shown by Rose [1963]. For some applications
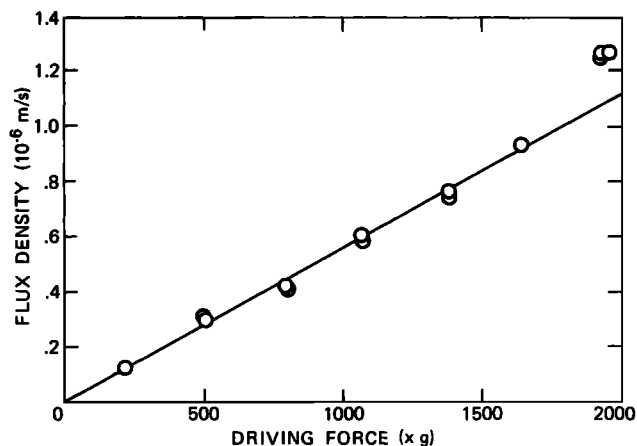
Fig. 11. Flux density versus total driving force measured for Oakley sand at water content 0.0878 m³ water/m³. The line is a least squares regression on all points at 1650 g or less.

the exclusion of vapor flow is desirable, as in the study of solute transport by the liquid phase.

Results achieved so far depend on the fact that the characteristics of the sample medium lead to effectively uniform moisture profiles, thus permitting easy justification of simplifying assumptions. More development, especially on the matter of ψ-profile determination, is needed to extend the method to other classes of materials. To extend the method to lower K values, it will be necessary to develop modifications of the flux-regulating apparatus and to change the sample geometry so that valid measurements can be made at greater accelerations. When these problems are solved, the steady state centrifuge method could be applicable to a wide variety of important problems in hydrology and other fields, for example, the measurement of aquifer recharge rates.

APPENDIX A: STEADY STATE PROFILE SHAPES

In this appendix we consider several constraints on the shape of steady state centrifuge $\psi(r)$ profiles, especially as they affect experimental considerations. The main questions to be answered concern which shape elements (Figure 2) are possible, how they can be combined, what conditions might lead to overall curve shapes that are nearly linear as desired for simple K measurements, what the slope of the profile would be in a region where it is essentially linear, and how certain parameters influence the profile.

Several relevant conditions either are known from the definition of the problem or are assumed from unsaturated flow theory. The flux density q is constant and positive (in the positive r direction). In the range of interest, $K(\psi)$ is positive and monotone increasing. The profile $\psi(r)$ is taken to be a solution of Darcy's law (2). Derivatives of ψ may then be written as

$$\psi' = \frac{d\psi}{dr} = \rho\omega^2 r - \frac{q}{K} \tag{A1}$$

$$\psi'' = \frac{d^2\psi}{dr^2} = \rho\omega^2 + q\frac{(dK/d\psi)}{K^2}\psi' = \rho\omega^2 + qJ\psi' \tag{A2}$$

where

$$J = J(\psi) = -\frac{d(K^{-1})}{d\psi} = \frac{dK/d\psi}{K^2} \tag{A3}$$

is a property of the porous medium and is always positive.

The physical situation referred to is that of Figure 1. It is assumed that $\psi_b = \psi(r_b)$ is a fixed boundary condition. Because this is the maximum r value of interest, most of the discussion concerns what shape the profile assumes as one considers r decreasing from r_b or some other value of r in the sample.

One simple constraint on the steady state (positive flux) profile is that its ψ values must be greater than those of the equilibrium (zero flux) $\psi(r)$ profile of (4), a result of the fact that the addition of water can make the soil wetter but not drier. For an unsaturated sample then the steady state profile will lie between the equilibrium $\psi(r)$ and $\psi(r) = 0$.

Of the seven shape elements in Figure 2, it is easily shown that elements D, E, and F are impossible. These cases have $\psi' \geq 0$, which means that the right-hand side of (A2) must be positive. Thus we have $\psi'' > 0$, contradicting the definitions of these shape elements.

Shape element G, with $\psi' > 0$, has both terms of (A2) positive. Therefore ψ' always decreases as r decreases, and if the

sample is long enough, ψ' would have to either become negative or asymptotically approach a nonnegative constant. If ψ' were to remain nonnegative, then ψ'' as given by (A2) would remain greater than or equal to $\rho\omega^2$, and ψ' could not approach a constant. The only remaining possibility is for ψ' to become negative. With ψ'' remaining positive at the point of transition, shape element G leads to shape element C.

Shape element B, with $\psi'' = 0$, requires

$$\psi' = -\frac{\rho\omega^2}{qJ} \tag{A4}$$

In this case we have

$$\psi'' = \frac{\rho\omega^2\psi'}{q}\frac{d(J^{-1})}{d\psi} \tag{A5}$$

For these two equations to be valid, J must be constant, implying $d(J^{-1})/d\psi = 0$. In certain experiments and in numerical calculations for certain realistic conditions, we have found that the magnitude of ψ'' over portions of shape elements A and C may be much smaller than relevant measurement errors, so that the assumption of a constant gradient is valid for the purpose of reducing experimental data. This is the condition that holds in the constant-gradient region referred to in the main text. In some of these cases it is also true that the mangitude of ψ' is small enough, compared to measurement errors, that it may be assumed to equal zero (shape element D).

Assuming slope continuity of the profile, the only possible binary couplings of elements are AC, CA, and GC (where the first of the two elements is the "lower" portion, at greater r). It would be useful to establish other constraints on profile shape, such as limitations on the length of the constant-gradient region and on the number of possible alternations of shape elements A and C; but for the most part, these depend on the specific nature of the $K(\psi)$ function.

In general, the value of ψ_b only has a significant influence on the lower part of the profile, near r_b. Consider two profiles $\psi_1(r)$ and $\psi_2(r)$, with $\psi_{b1} > \psi_{b2}$ and all other parameters the same. Because (2) has only one solution for a given boundary condition, if ψ_1 and ψ_2 have the same value at a point, they agree for all r. Therefore $\psi_1(r)$ and $\psi_2(r)$ cannot cross or touch. Then since $\psi_1(r) > \psi_2(r)$ and $K(\psi)$ is monotone increasing, we know from (A1) that $\psi_1' > \psi_2'$ and hence $d(|\psi_1 - \psi_2|)/dr > 0$. This condition implies that the two curves approach each other as r decreases. The curves could fail to approach a common limit only for the case of constant $K(\psi)$. For the typical case shown in Figure 5, the curves are for practical purposes the same for r less than a certain value.

The effect of changes in ω on the slope of the profile in the constant-gradient region becomes negligible as ω increases. When ω is large enough, as specified in Appendix B, q may be assumed proportional to ω^2. Then the "constant" ψ given by (A4) depends only on J. For a given sample, ψ' will then be effectively independent of ω. It may also be noted that for smaller magnitudes of ψ', $J(\psi)$ will vary less with r, and ψ' will be more nearly constant. Thus a small magnitude of slope goes with a small curvature of the profile.

APPENDIX B: PREDICTION OF FLUX DENSITY

In the numerical model for predicting $\psi(r)$ profiles, flux density q is an input parameter. The value of q is one of the measured quantities determined in a steady state experiment. For use of the numerical model in trial predictions it is neces-

sary to estimate q from characteristics of the apparatus and operating conditions to be employed.

The flux is established by means of a height h of water above a saturated ceramic plate used as an impeding layer above the top of the sample as shown in Figure 1. It is desirable to predict q in terms of the saturated conductivity of the ceramic plate K_c, the plate thickness l, and the radial distances r_{cw} and r_{wa}. Equation (2) can be applied to the ceramic plate and integrated from r_{cw} to r_t to get

$$q = -\frac{K_c}{l}\left[\psi_t - \psi(r_{cw}) - \rho\omega^2 l r_c\right] \qquad (B1)$$

where $\psi_t = \psi(r_t)$ represents the pressure at the top of the sample (bottom of the ceramic) and r_c is the radius to the midpoint of the ceramic plate, $(r_t + r_{cw})/2$. The second term in brackets represents the pressure at the top of the ceramic. Because this pressure is generated solely by the static water column above the plate, it is readily computed by (4), so that q can be determined from

$$q = -\frac{K_c}{l}\left[\psi_t + \rho\omega^2\left(\frac{r_{wa}^2 - r_{cw}^2}{2}\right) - \rho\omega^2 l r_c\right] \qquad (B2)$$

The second and third terms in brackets are determined directly from known quantities, but the first, ψ_t, is determined (in the absence of measurements) only as a result of the profile-model calculation. When ω is large enough that the second and third terms dominate, we can ignore ψ_t and use the approximate relation

$$q = -K_c\rho\omega^2\left[\frac{r_{wa}^2 - r_{cw}^2}{2l} - r_c\right] \qquad (B3)$$

Under these conditions, q is effectively proportional to ω^2.

For ω small enough to require (B2), the profile-model calculation can be done initially with a guess of the value of ψ_t. From the new value of ψ_t in the resulting $\psi(r)$ profile, a new value of q can be determined for use in a repetition of the model calculation. If necessary, further iteration should produce successive ψ_t values that are sufficiently close together.

For the curves in Figures 3 and 4, q was computed using (B2), starting with a ψ_t value of -19.6 kPa and iterating according to the procedure described above until successive ψ_t values differed by less than 0.1 kPa. No more than three iterations were required. K_c values were 1.00×10^{-10} m/s (15-bar ceramic) for curve F of Figure 3 and 3.80×10^{-10} m/s (5-bar ceramic) for the other curves.

The validity of (B2) may be tested by comparison with actual measured q values under known conditions. In cases examined so far, agreement between measured and calculated fluxes has not always been very close, though always within a factor of 2. Probably the greatest difficulty here is that the ceramic plate conductivity K_c was measured several months before the time of the experiment and so may have changed appreciably. Another way to test (B2) is by measuring q for two different values of height h of water above the applicator plate. If the comparison is between ratios of q values, experimental and theoretical, then K_c is irrelevant as long as it is the same for the two measurements. At $\omega = 105$ s^{-1}, two brief runs with h equal to 3.2 and 8.7 mm had fluxes in the ratio 1.33, while (5) predicts 1.22. In a test at $\omega = 314$ s^{-1}, average q values for two complete series of three or more runs with h equal to 8.8 and 13.3 mm were in the ratio 1.25, very close to the prediction 1.24. Errors were much smaller in the second

test because ψ_t is negligible at the higher speed and the 40-fold greater total volume of flux produced more accurate q values.

NOTATION

g acceleration of gravity at earth's surface.
J symbol for $-d(K^{-1})/d\psi$.
K hydraulic conductivity.
K_c hydraulic conductivity of ceramic plate.
K_{sat} saturated hydraulic conductivity.
n exponent in Gardner empirical formula for $K(\psi)$.
q flux density.
r radius from center of rotation.
r_b value of r at bottom of sample (lower boundary).
r_t value of r at top of sample.
θ volumetric water content.
ρ density of liquid.
ψ matric potential.
ψ' first derivative of $\psi(r)$, $d\psi/dr$.
ψ'' second derivative of $\psi(r)$, $d^2\psi/dr^2$.
ψ_0 ψ scale factor in Gardner empirical formula for $K(\psi)$.
ψ_b boundary condition for ψ at $r = r_b$.
ψ_t value of ψ at top of sample, $\psi(r_t)$.
ω angular speed.

REFERENCES

Alemi, M. H., D. R. Nielsen, and J. W. Biggar, Determining the hydraulic conductivity of soil cores by centrifugation, *Soil. Sci. Soc. Am. Proc.*, *40*, 212–218, 1976.

Bear, J., M. Y. Corapcioglu, and J. Balakrishna, Modeling of centrifugal filtration in unsaturated deformable porous media, *Adv. Water Resour.*, *7*, 150–167, 1984.

Briggs, L. J., and J. W. McLane, The moisture equivalent of soils, *U.S. Dep. Agric. Bur. Soils Bull.*, *45*, 1907.

Childs, E. C., and N. Collis-George, The permeability of porous materials, *Proc. R. Soc. London, Ser. A*, *201*, 392–405, 1950.

Gardner, R., A method of measuring the capillary tension of soil moisture over a wide moisture range, *Soil Sci.*, *43*, 277, 1937.

Gardner, W. R., Water movement below the root zone, *Trans. Int. Congr. Soil Sci. 8th*, *1964*, 63–68, 1964.

Hadas, A., Deviations from Darcy's law for the flow of water in unsaturated soils, *Israel J. Agric. Res.*, *14*(4), 159–168, 1964.

Hagoort, J., Oil recovery by gravity drainage, *Soc. Pet. Eng. J.*, *20*, 139–150, 1980.

Hassler, G. L., and E. Brunner, Measurement of capillary pressures in small core samples, *Trans. Am. Inst. Min. Metall. Pet. Eng.*, *160*, 114–123, 1945.

Henrici, P., *Elements of Numerical Analysis*, p. 275, John Wiley, New York, 1964.

Hillel, D., and W. R. Gardner, Measurement of unsaturated conductivity and diffusivity by infiltration through an impeding layer, *Soil Sci.*, *109*, 149–153, 1970.

Kisch, M., The theory of seepage from clay-blanketed reservoirs, *Geotechnique*, *9*, 9–21, 1959.

Mualem, Y., and A. Klute, A predictor-corrector method for measurement of hydraulic conductivity and membrane conductance, *Soil Sci. Soc. Am. J.*, *48*, 993–1000, 1984.

Olson, T. C., and D. Swartzendruber, Velocity-gradient relationships for steady-state unsaturated flow of water in nonswelling artificial soils, *Soil Sci. Soc. Am. Proc.*, *32*, 457–462, 1968.

Richards, L. A., Capillary conduction of liquids through porous mediums, *Physics*, *1*, 318–333, 1931.

Ripple, C. D., R. V. James, and J. Rubin, Radial particle-size segregation during packing of particulates into cylindrical containers, *Powder Technol.*, *8*, 165–175, 1973.

Rose, D. A., Water movement in porous materials, 2, The separation of the components of water movement, *Br. J. Appl. Phys.*, *14*, 491–496, 1963.

Rubin, J., Theoretical analysis of two-dimensional, transient flow of water in unsaturated and partly unsaturated soils, *Soil Sci. Soc. Am. Proc., 32,* 607–615, 1968.

Rubin, J., and R. Steinhardt, Soil-water relations during rain infiltration, 1, Theory, *Soil Sci. Soc. Am. Proc., 27,* 246–251, 1963.

Rubin, J., R. Steinhardt, and P. Reiniger, Soil water relations during rain infiltration, 2, Moisture content profiles during rains of low intensities, *Soil. Sci. Soc. Am. Proc., 28,* 1–5, 1964.

Russell, M. B., and L. A. Richards, The determination of soil moisture energy relations by centrifugation, *Soil Sci. Soc. Am. Proc., 3,* 65–69, 1938.

Stewart, B. A., F. G. Viets, G. L. Hutchinson, W. D. Kemper, F. E. Clark, M. L. Fairbourn, and F. Strauch, Distribution of nitrates and other water pollutants under fields and corrals in the Middle South Platte Valley of Colorado, *USDA-ARS 41-134,* p. 8, U.S. Dep. of Agric., Washington, D. C., 1967.

Stonestrom, D. A., Co-determination and comparison of hysteresis-affected, parametric functions of unsaturated flow: Water-content dependence of matric pressure, air trapping, and fluid permeabilities in a non-swelling soil, Ph.D. thesis, Stanford Univ., Stanford, Calif., 1986.

Swartzendruber, D., Non-Darcy behavior and the flow of water in unsaturated soils, *Soil. Sci. Am. Proc., 27,* 491–495, 1963.

Thames, J. L., and D. D. Evans, An analysis of the vertical infiltration of water into soil columns, *Water Resour. Res., 4,* 817–828, 1968.

Veihmeyer, F. J., O. W. Israelsen, and J. P. Conrad, The moisture equivalent as influenced by the amount of soil used in its determination, *Tech. Pap. 16,* Univ. of Calif., Coll. of Agric., Berkeley, 1924.

Watson, K. K., An instantaneous profile method for determining the hydraulic conductivity of unsaturated porous materials, *Water Resour. Res., 2,* 709–715, 1966.

Youngs, E. G., An infiltration method of measuring the hydraulic conductivity of unsaturated porous materials, *Soil Sci., 97,* 307–311, 1964.

D. P. Hammermeister, J. R. Nimmo, and J. Rubin, U.S. Geological Survey, 345 Middlefield Road, MS-421, Menlo Park, CA 94025.